# Fast Bayesian approach for modal identification using free vibration data, Part I – Most probable value

Feng-Liang Zhang[1], Yan-Chun Ni[1*], Siu-Kui Au[2] and Heung-Fai Lam[3]

[1]Research Institute of Structural Engineering and Disaster Reduction, College of Civil Engineering, Tongji University, 1239 Siping Road, Shanghai, China
[2]Center for Engineering Dynamics and Institute for Risk and Uncertainty, University of Liverpool, L69 3GH, Liverpool, United Kingdom
[3]Department of Civil and Architectural Engineering, City University of Hong Kong, 83 Tat Chee Avenue, Kowloon, Hong Kong

**Abstract:** The identification of modal properties from field testing of civil engineering structures is becoming economically viable, thanks to the advent of modern sensor and data acquisition technology. Its demand is driven by innovative structural designs and increased performance requirements of dynamic-prone structures that call for a close cross-checking or monitoring of their dynamic properties and responses. Existing instrumentation capabilities and modal identification techniques allow structures to be tested under free vibration, forced vibration (known input) or ambient vibration (unknown broadband loading). These tests can be considered complementary rather than competing as they are based on different modeling assumptions in the identification model and have different implications on costs and benefits. Uncertainty arises naturally in the dynamic testing of structures due to measurement noise, sensor alignment error, modeling error, etc. This is especially relevant in field vibration tests because the test condition in the field environment can hardly be controlled. In this work, a Bayesian statistical approach is developed for modal identification using the free vibration response of structures. A frequency domain formulation is proposed that makes statistical inference based on the Fast Fourier Transform (FFT) of the data in a selected frequency band. This significantly simplifies the identification model because only the modes dominating the frequency band need to be included. It also legitimately ignores the information in the excluded frequency bands that are either irrelevant or difficult to model, thereby significantly reducing modeling error risk. The posterior probability density function (PDF) of the modal parameters is derived rigorously from modeling assumptions and Bayesian probability logic. Computational difficulties associated with calculating the posterior statistics, including the most probable value (MPV) and the posterior covariance matrix, are addressed. Fast computational algorithms for determining the MPV are proposed so that the method can be practically implemented. In the companion paper (Part II), analytical formulae are derived for the posterior covariance matrix so that it can be evaluated without resorting to finite difference method. The proposed method is verified using synthetic data. It is also applied to modal identification of full-scale field structures.

**Keywords:** Free vibration, Bayesian, FFT, modal identification, field test

---

[*] Corresponding author. Tel.: +86 021 65987352; E-mail address: yanchunni@gmail.com

## 1. Introduction

Modern sensor and data acquisition technology have allowed structural responses to be practically measured with reasonable quality. The vibration data of an as-built structure can be used for identifying its ‘modal properties’, which primarily consist of the natural frequencies, damping ratios and mode shapes. The modal properties are indispensable for structural health monitoring, model updating and damage detection [1][2][3]. Three types of tests are commonly performed for obtaining vibration data for modal identification. In an ambient vibration test, vibration data is obtained when the structure is in its working condition without artificial loading [4][5][6]. The input ambient loading arising from the environment and operational activities is not measured but is assumed to be broadband random. Economy is a significant advantage, although the signal-to-noise (s/n) ratio and hence the identification possibility/quality cannot be directly controlled. In a forced vibration test, artificial known excitation is applied to the structure [7][8][9][10]. The vibration level and hence the s/n ratio can be directly controlled and enhanced significantly. It is often more expensive because special equipment such as a high-payload shaker is needed and greater risk management is required. In a free vibration test, vibration data is obtained when the structure is dominantly under free vibration. Although it still requires artificial excitation to initiate vibration of the structure to an adequate level, such excitation need not be measured and so it allows greater flexibility and puts less demand on equipment.

Many modal identification approaches using free vibration data have been developed. The Ibrahim time domain method (ITD) makes use of generalized eigenvalue decomposition [11][12][13]. It was originally developed for displacement response data but later generalized for velocity and acceleration data through a state-space formulation [11][13]. The complex exponential method makes use of singular value decomposition [14]. The least square method is conceptually straightforward and it identifies the set of modal parameters as the one that minimizes a measure of fit between the theoretical and measured response in a least square sense [15][16].

Proper orthogonal decomposition or the so-called Karhunen Loeve decomposition was used for statistical analysis of free vibration response data and identifying the mode shape vectors [17]. It was later applied to response data under free vibration and harmonic excitations [18]. It was also applied to obtain proper orthogonal modes under proportionality assumption on the mass matrix [19]. The constraint was later removed, leading to the method MAFVFO (Modal Analysis by using Free Vibration Response Only) [20]. Based on the measured data, other kinematic quantities (e.g., displacement, velocity, acceleration) consistent with the data are determined by numerical differentiation/integration and are subsequently used for modal identification. The method is applicable for discrete and continuous mass systems and it has been extended to treat non-proportional damping [21].

Methods based on wavelet transforms have also been developed. Discrete wavelet transform (DWT) was combined with the Hilbert transform to determine the natural frequencies and damping ratios of a structure [22]. It was later extended to analyze free vibration response and earthquake response, where the equations of motion were determined by DWT to identify the modal parameters corresponding to different kinds of mother wavelet functions [23]. One drawback of DWT is its computational inefficiency. In view of this, methods based on continuous wave transform (CWT) were developed for modal identification based on the modulus and phase of the transform [24][25][26]. The Hilbert–Huang transformation [27], a general method for analyzing nonlinear and non-stationary signal analysis, has also been applied to modal identification with free vibration data for linear and nonlinear systems [28][29].

Despite the abundance of the aforementioned methods, they are based on empirical statistical proxies (e.g., correlation functions) for identification and they do not account for the identification uncertainty of the modal parameters. The former implies that the method may not have utilized all information in the data for identification. The latter is especially relevant for field vibration data as there is less control on the test condition compared to laboratory data. In free vibration field tests, the measured data mainly consists of three parts: free vibration response, measurement noise and ambient vibration response. Existing identification methods often assume that the first two components dominate the measured data and ignore the effect of the last component. In reality, arising from the measurement noise and ambient component, the measured data exhibits a variety of spectral characteristics over its sampling bandwidth (i.e., up to the Nyquist frequency), many of which are irrelevant to the modes to be identified or are difficult to model. These issues call for a careful choice of assumptions in the identification model and a fundamental formulation to account for uncertainty. Otherwise it may lead to significant bias or conclusions inconsistent with structural dynamics.

In this work, a Bayesian statistical method based on the Fast Fourier Transform (FFT) of free vibration data is developed. It exploits the statistical properties of the FFT data to construct a posterior probability density function (PDF), providing a fundamental means for identifying the modal parameters as well as their uncertainty consistent with probability logic and modeling assumptions. As is common in Bayesian methods, computational difficulties are encountered when determining the posterior MPV and the associated covariance matrix. From first principles, determining the MPV requires solving a numerical optimization problem whose dimension grows linearly with the number of measured degrees of freedom (dofs). In view of this, computational strategies are developed by exploiting the mathematical structure of the problem in well-separated and closely-spaced mode situations. In the companion paper, the posterior covariance matrix of the modal parameters is investigated, where closed-form analytical expressions are derived for evaluation without resorting to finite difference method. Examples with synthetic data are also provided to verify the proposed theory. Field test data are used to illustrate the practical application of the method.

## 2. Bayesian FFT modal identification

Consider a structure initially excited by some artificial means and then left to vibrate 'freely'. The measured (acceleration) data $\ddot{\mathbf{y}}_j \in R^n \, (j = 1,\ldots,N)$ during the free vibration phase generally consists of free vibration response $\ddot{\mathbf{x}}_{\mathrm{f}j}$ due to the initial artificial excitation, ambient vibration response $\ddot{\mathbf{x}}_{\mathrm{a}j}$ due to unknown environmental disturbance and prediction error $\boldsymbol{\varepsilon}_j$:

$$\ddot{\mathbf{y}}_j = \ddot{\mathbf{x}}_{\mathrm{f}j} + \ddot{\mathbf{x}}_{\mathrm{a}j} + \boldsymbol{\varepsilon}_j \qquad (1)$$

where $N$ is the number of sampling points; $n$ is the number of measured dofs. The prediction error accounts for the discrepancy between the measured response and the (theoretical) model response for given modal parameters. The FFT of $\ddot{\mathbf{y}}_j$ is defined as

$$\mathcal{F}_k = \sqrt{\frac{2\Delta t}{N}} \sum_{j=1}^{N} \ddot{\mathbf{y}}_j \exp[-2\pi \mathbf{i} \frac{(k-1)(j-1)}{N}] \qquad (k = 1,\ldots,N) \qquad (2)$$

where $\mathbf{i}^2 = -1$; $\Delta t$ is the sampling interval. For $k = 2,3,..., N_q$, the FFT corresponds to frequency $\mathrm{f}_k = (k-1)/N\Delta t$, with $N_q$ being the frequency index at the Nyquist frequency, and equal to the integer part of $N/2+1$. Let

$$\mathbf{Z}_k = [\mathrm{Re}\mathcal{F}_k; \mathrm{Im}\mathcal{F}_k] \in R^{2n} \tag{3}$$

be an augmented vector of the real and imaginary parts of the FFT. In practice, only the FFT data confined to a selected frequency band dominated by the target mode(s) are used for statistical inference. Such FFT data are denoted by $\{\mathbf{Z}_k\}$.

Let $\boldsymbol{\theta}$ denote the set of modal parameters to be identified, which includes four groups of parameters. The first group is $\{f_i, \zeta_i, \boldsymbol{\Phi}(i) : i = 1,..., m\}$, where $f_i$ and $\zeta_i$ denote the natural frequency and damping ratio of the $i$-th mode, respectively; $\boldsymbol{\Phi}(i) \in R^n$ is the $i$-th mode shape vector confined to the measured dofs $n$; $m$ is the number of modes to be identified. The second group is $\{u_i, v_i : i = 1,..., m\}$, where $u_i$ and $v_i$ are the initial acceleration and its derivative of the $i$-th modal free vibration response, respectively. The third group is $\mathbf{S} \in R^{m \times m}$, the (Hermitian) power spectral density (PSD) matrix of modal forces of ambient vibration response. The fourth one is $S_e$, the PSD of prediction error (assuming independent and identically distributed channel noise). The ambient modal force and the prediction error are assumed to have a constant PSD in the selected frequency band. Note that in the ambient modal identification, the input excitation is usually assumed to be white noise, which corresponds to a constant PSD of modal force for all frequencies up to Nyquist frequency. In the proposed method, only the PSD is assumed constant in the resonance band of the mode only, which is often narrow. This assumption is less stringent and hence more robust. For the prediction error, since it mainly comes from measurement noise or modelling error, it is reasonable to be assumed as independent and identically distributed (i.i.d.) Gaussian white noise. The assumption for PSD of modal force and PSD of prediction error can also be referred to [30][31].

Using Bayes' Theorem, the posterior PDF of $\boldsymbol{\theta}$ given the data is given by:

$$p(\boldsymbol{\theta} | \{\mathbf{Z}_k\}) \propto p(\boldsymbol{\theta}) p(\{\mathbf{Z}_k\} | \boldsymbol{\theta}) \tag{4}$$

where $p(\boldsymbol{\theta})$ is the prior PDF that reflects the plausibility of $\boldsymbol{\theta}$ in the absence of data. Assuming a constant prior PDF (i.e., uninformative), the posterior PDF $p(\boldsymbol{\theta} | \{\mathbf{Z}_k\})$ is directly proportional to the 'likelihood function' $p(\{\mathbf{Z}_k\} | \boldsymbol{\theta})$.

The likelihood function can be derived based on the following observations. First note that for a given $\boldsymbol{\theta}$ the free vibration response $\ddot{\mathbf{x}}_{fj}(\boldsymbol{\theta})$ can be determined and hence is fixed. It then follows from (1) that the difference $\ddot{\mathbf{y}}_j - \ddot{\mathbf{x}}_{fj}(\boldsymbol{\theta})$ is distributed as the ambient vibration response with prediction error, whose statistical properties have been respectively specified by $\mathbf{S}$ and $S_e$ (contained in $\boldsymbol{\theta}$). For a given $\boldsymbol{\theta}$ the difference $\ddot{\mathbf{y}}_j - \ddot{\mathbf{x}}_{fj}(\boldsymbol{\theta})$ is then a zero-mean stationary stochastic process, where for large $N$ its FFTs at different frequency indices are asymptotically independent and jointly Gaussian [32]. Their covariance matrix can also be derived analytically using random vibration theory, giving a closed-form expression in terms of the modal properties. In summary, for a given $\boldsymbol{\theta}$, $\{\mathbf{Z}_k\}$ are independent and jointly Gaussian. Each $\mathbf{Z}_k$ has mean $\boldsymbol{\mu}_k(\boldsymbol{\theta}) \in R^{2n}$ given by the FFT of free vibration response and covariance matrix $\mathbf{C}_k(\boldsymbol{\theta}) \in R^{2n\times 2n}$ given by the ambient response and prediction error. Consequently, the likelihood function is given by:

$$p(\{\mathbf{Z}_k\} | \boldsymbol{\theta}) = \prod_k (2\pi)^{-n} (\det \mathbf{C}_k(\boldsymbol{\theta}))^{-1/2} \exp\{-\frac{1}{2}[\mathbf{Z}_k - \boldsymbol{\mu}_k(\boldsymbol{\theta})]^T \mathbf{C}_k^{-1}(\boldsymbol{\theta})[\mathbf{Z}_k - \boldsymbol{\mu}_k(\boldsymbol{\theta})]\} \tag{5}$$

where $\det(.)$ denotes the determinant; $\boldsymbol{\mu}_k(\boldsymbol{\theta}) = \mathrm{E}[\mathbf{Z}_k | \boldsymbol{\theta}]$ with $\mathrm{E}[\cdot | \boldsymbol{\theta}]$ denoting the conditional expectation for a given $\boldsymbol{\theta}$; $\mathbf{C}_k(\boldsymbol{\theta})$ is the covariance matrix of $\mathbf{Z}_k$ [33]:

$$\mathbf{C}_k(\boldsymbol{\theta}) = \frac{1}{2}\begin{bmatrix} \boldsymbol{\Phi}\,\mathrm{Re}\,\mathbf{H}_k\boldsymbol{\Phi}^T & -\boldsymbol{\Phi}\,\mathrm{Im}\,\mathbf{H}_k\boldsymbol{\Phi}^T \\ \boldsymbol{\Phi}\,\mathrm{Im}\,\mathbf{H}_k\boldsymbol{\Phi}^T & \boldsymbol{\Phi}\,\mathrm{Re}\,\mathbf{H}_k\boldsymbol{\Phi}^T \end{bmatrix} + \frac{S_e}{2}\mathbf{I}_{2n} \tag{6}$$

Here, $\boldsymbol{\Phi} = [\boldsymbol{\Phi}(1), \boldsymbol{\Phi}(2), ..., \boldsymbol{\Phi}(m)] \in R^{n\times m}$ is the mode shape matrix; $\mathbf{I}_{2n} \in R^{2n\times 2n}$ denotes the identity matrix; $\mathbf{H}_k \in C^{m\times m}$ is a transfer matrix whose ($i$, $j$) element is given by

$$\mathbf{H}_k(i, j) = S_{ij}[(\beta_{ik}^2 - 1) + 2\mathbf{i}\zeta_i\beta_{ik}]^{-1}[(\beta_{jk}^2 - 1) - 2\mathbf{i}\zeta_j\beta_{jk}]^{-1} \tag{7}$$

where $S_{ij}$ is the ($i$, $j$) element of the PSD matrix of modal force $\mathbf{S}$ due to ambient excitation; $\beta_{ik} = f_i / \mathrm{f}_k$; $\mathrm{f}_k$ is the FFT frequency abscissa.

The expression for $\boldsymbol{\mu}_k(\boldsymbol{\theta})$ can be derived as follows. The acceleration of free vibration response is given by

$$\ddot{\mathbf{x}}_{\mathrm{f}}(t) = \sum_{i=1}^{m} \boldsymbol{\Phi}(i) \ddot{\eta}_{fi}(t) \tag{8}$$

where $\ddot{\eta}_{fi}(t)$ is the $i$-th modal acceleration of free vibration response satisfying:

$$\ddot{\eta}_{fi}(t) + 2\zeta_i \omega_i \dot{\eta}_{fi}(t) + \omega_i^2 \eta_{fi}(t) = 0 \tag{9}$$

and $\zeta_i$ is the damping ratio; $\omega_i = 2\pi f_i$ is the natural frequency (in rad/s) of the $i$-th mode. Differentiating (9) twice gives again a homogeneous second-order differential equation of the variable $z_i(t) = \ddot{\eta}_{fi}(t)$, solving which yields

$$\ddot{\eta}_{fi}(t) = u_i g_{1i}(t) + v_i g_{2i}(t) \tag{10}$$

where $u_i = \ddot{\eta}_{fi}(0)$ and $v_i = \dddot{\eta}_{fi}(0)$;

$$g_{1i}(t) = e^{-\zeta_i \omega_i t} (\cos \omega_{di} t + \frac{\zeta_i}{\sqrt{1-\zeta_i^2}} \sin \omega_{di} t) \tag{11}$$

$$g_{2i}(t) = \frac{e^{-\zeta_i \omega_i t}}{\omega_{di}} \sin \omega_{di} t \tag{12}$$

and $\omega_{di} = \omega_i \sqrt{1-\zeta_i^2}$. Note that $g_{1i}$ is the familiar single dof free vibration response with unit initial displacement and zero velocity; $g_{2i}$ is the one with zero initial displacement and unit velocity.

Substituting (10) into (8) gives:

$$\ddot{\mathbf{x}}_{\mathrm{f}}(t) = \sum_{i=1}^{m} \boldsymbol{\Phi}(i) \left[ u_i g_{1i}(t) + v_i g_{2i}(t) \right] \tag{13}$$

For a given $\boldsymbol{\theta}$, $\boldsymbol{\mu}_k(\boldsymbol{\theta})$ can then be obtained as an augmented vector of the real and imaginary parts of the FFT of $\ddot{\mathbf{x}}_f$. Note that $g_{1i}$ and $g_{2i}$ depend on $\boldsymbol{\theta}$ through the natural frequency and damping ratio. The parameters $u_i$ and $v_i$ specify the initial conditions of the free vibration component of the modal response only. They do not completely specify the initial conditions of the total modal response because the latter contains ambient vibration components which are unknown.

To determine the MPV of the modal parameters, the likelihood function in (5) should be maximized. This is equivalent to minimizing the 'negative log-likelihood function' (NLLF):

$$\begin{aligned} L(\boldsymbol{\theta}) &= -\ln p(\{\mathbf{Z}_k\} \mid \boldsymbol{\theta}) \\ &= nN_f \ln 2 + nN_f \ln \pi + \frac{1}{2}\sum_k \ln\det \mathbf{C}_k(\boldsymbol{\theta}) + \frac{1}{2}\sum_k \left[\mathbf{Z}_k - \boldsymbol{\mu}_k(\boldsymbol{\theta})\right]^T \mathbf{C}_k(\boldsymbol{\theta})^{-1}\left[\mathbf{Z}_k - \boldsymbol{\mu}_k(\boldsymbol{\theta})\right] \end{aligned} \tag{14}$$

Direct numerical minimization of the NLLF is infeasible for two basic reasons [34]. First, $\mathbf{C}_k(\boldsymbol{\theta})$ in (6) is close to being rank deficient (especially for good quality data) because it is dominated by the first term whose rank is at most 2m. Second, and more importantly, the number of parameters to be optimized, which is equal to the number of modal parameters in $\boldsymbol{\theta}$, can be quite large in applications. Specifically, taking into account the Hermitian nature of the PSD matrix of modal force $\mathbf{S}$, the number of parameters in $\boldsymbol{\theta}$ is equal to

$$n_p = 4m + mn + m^2 + 1 \tag{15}$$

The growth of $n_p$ with the number of measured dofs $n$ is a major issue because the latter can be moderate to large in applications. For example, measuring tri-axially six locations and identifying two modes in a band gives $n = 18$, $m = 2$ and $n_p = 49$. The growth of $n_p$ with the number of modes $m$ is a secondary issue because $m$ only needs to include the modes in the selected frequency band, i.e., closely-spaced modes, which rarely exceeds three.

In the remainder of this paper, we shall develop efficient methods for determining the MPV of the modal parameters. The development is separated into two cases, namely, well-separated modes and general multiple (possibly closely-spaced) modes. In the first case it is possible to obtain an analytical solution for the most probable mode shape, which in turn allows a very fast iterative procedure. The case of general multiple modes (i.e., second case) is more complicated and it has not been possible to obtain an analytical solution for the most probable mode shape. To explore fast solutions, we consider the case when the ambient vibration component can be ignored (but measurement noise is still present). It turns out that in this case, the most probable mode shape can be determined analytically, which again results in an efficient algorithm for Bayesian modal identification.

Note that the methods proposed are the extension of the work in [34]. As mentioned, in reality, the measured free vibration response consists of free vibration and ambient vibration responses. Since the free vibration response can be determined given modal parameters and is fixed, the difference between measured response and free vibration response will be distributed as the ambient vibration response with prediction error, based on which, a similar likelihood function can be constructed as shown in equation (14).

## 3. Well-separated modes

For well-separated modes, one can select a frequency band that is determined by a single mode of interest, so that m=1. In this case, the set of modal parameters $\boldsymbol{\theta}$ consists of the natural frequency $f$, damping ratio $\zeta$, mode shape vector $\boldsymbol{\varphi} \in R^n$, PSD of modal force $S$, PSD of prediction error $S_e$ and the initial modal acceleration $u$ and its derivative $v$. For simplicity in notation, we have dropped the mode index.

### 3.1. Reformulation of NLLF

We reformulate the NLLF in (14) in order to facilitate deriving the most probable mode shape, the MPV of initial modal acceleration $u$ and its derivative $v$. The idea is to rewrite the NLLF as a quadratic form of the mode shape vector $\boldsymbol{\varphi}$. Note that $\boldsymbol{\varphi}$ affects $\mathbf{C}_k(\boldsymbol{\theta}) \in R^{2n\times 2n}$ and $\boldsymbol{\mu}_k(\boldsymbol{\theta}) \in R^{2n}$. Using eigenvector decomposition, the determinant and inverse of $\mathbf{C}_k(\boldsymbol{\theta})$ have been shown to be [34]:

$$\det\mathbf{C}_k(\boldsymbol{\theta}) = 2^{-2n}[(SD_k / S_e + 1)S_e^n]^2 \tag{16}$$

$$\mathbf{C}_k^{-1}(\boldsymbol{\theta}) = 2\begin{bmatrix} S_e^{-1}\mathbf{I}_n - S_e^{-1}(1+S_e/SD_k)^{-1}\boldsymbol{\varphi}\boldsymbol{\varphi}^T & \mathbf{0} \\ \mathbf{0} & S_e^{-1}\mathbf{I}_n - S_e^{-1}(1+S_e/SD_k)^{-1}\boldsymbol{\varphi}\boldsymbol{\varphi}^T \end{bmatrix} \tag{17}$$

where

$$D_k(f,\zeta) = [(\beta_k^2 - 1)^2 + (2\zeta\beta_k)^2]^{-1} \tag{18}$$

and $\beta_k = f/\mathrm{f}_k$. On the other hand, taking FFT on (13) and noting that the LHS is just $\boldsymbol{\mu}_k(\boldsymbol{\theta})$ gives

$$\boldsymbol{\mu}_k(\boldsymbol{\theta}) = \begin{bmatrix} \boldsymbol{\varphi} b_{\mathrm{R}k} \\ \boldsymbol{\varphi} b_{\mathrm{I}k} \end{bmatrix} \in R^{2n} \tag{19}$$

where $b_{\mathrm{R}k}$ and $b_{\mathrm{I}k}$ denote the real and imaginary parts of $b_k$, respectively; $b_k$ is the FFT of the modal free vibration acceleration and is equal to

$$b_k = \sqrt{\frac{2\Delta t}{N}} \sum_{j=1}^{N} [u g_1(t_j) + v g_2(t_j)] \exp[-2\pi \mathbf{i} \frac{(k-1)(j-1)}{N}] \qquad (k = 1,\ldots,N) \tag{20}$$

Here, $g_1$ and $g_2$ are given by (11) and (12) , respectively, with the mode index '$i$' omitted.

Substituting (16), (17) and (19) into (14) and using $\boldsymbol{\varphi}^T\boldsymbol{\varphi} = 1$ gives, after algebra,

$$\begin{aligned} L(\boldsymbol{\theta}) &= nN_f \ln\pi + (n-1)N_f \ln S_e + \sum_k \ln(SD_k + S_e) \\ &+ S_e^{-1}[d - \boldsymbol{\varphi}^T \mathbf{A}\boldsymbol{\varphi} + \sum_k (1-a_k)(b_{\mathrm{R}k}^2 + b_{\mathrm{I}k}^2) - 2\boldsymbol{\varphi}^T \sum_k (1-a_k)(b_{\mathrm{R}k} \operatorname{Re}\mathcal{F}_k + b_{\mathrm{I}k} \operatorname{Im}\mathcal{F}_k)] \end{aligned} \tag{21}$$

where

$$a_k = (1 + S_e/SD_k)^{-1} \tag{22}$$

$$d = \sum_k (\operatorname{Re}\mathcal{F}_k^T \operatorname{Re}\mathcal{F}_k + \operatorname{Im}\mathcal{F}_k^T \operatorname{Im}\mathcal{F}_k) \tag{23}$$

$$\mathbf{A} = \sum_k a_k (\operatorname{Re}\mathcal{F}_k \operatorname{Re}\mathcal{F}_k^T + \operatorname{Im}\mathcal{F}_k \operatorname{Im}\mathcal{F}_k^T) \tag{24}$$

The MPV of modal parameters minimizes the NLLF in (21) subject to the unit norm constraint:

$$\boldsymbol{\varphi}^T\boldsymbol{\varphi} = 1 \tag{25}$$

To incorporate this constraint, we consider the following objective function when determining the MPV of modal parameters:

$$J(\boldsymbol{\theta}) = L(\boldsymbol{\theta}) + \lambda(\boldsymbol{\varphi}^T\boldsymbol{\varphi} - 1) \tag{26}$$

where $\lambda$ is a Lagrange multiplier .

The significance of (21) is that it is a quadratic form of $\boldsymbol{\varphi}$. This allows the MPV of $\boldsymbol{\varphi}$ to be determined analytically, as shown next.

## 3.2. Partial analytical solution for mode shape $\boldsymbol{\varphi}$

Differentiating $J$ with respect to $\boldsymbol{\varphi}$ and setting it equal to zero yields

$$\mathbf{A}\boldsymbol{\varphi} + \mathbf{q} = S_e\lambda\boldsymbol{\varphi} \tag{27}$$

where

$$\mathbf{q} = \sum_k (1 - a_k)(b_{\mathrm{R}k}\,\mathrm{Re}\mathcal{F}_k + b_{\mathrm{I}k}\,\mathrm{Im}\mathcal{F}_k) \tag{28}$$

Here, (25) and (27) form a 'constrained eigenvalue problem'. It can be solved by defining an auxiliary vector which satisfies a standard eigenvalue problem [35][36][37] (details omitted here). As a result, the MPV of $\boldsymbol{\varphi}$ can be obtained as the upper half of the eigenvector (normalized to have unit norm) with the largest eigenvalue of the matrix $\mathbf{G} \in R^{2n\times 2n}$:

$$\mathbf{G} = \begin{bmatrix} \mathbf{A} & \mathbf{q}\mathbf{q}^T \\ \mathbf{I}_n & \mathbf{A} \end{bmatrix} \tag{29}$$

## 3.3. Partial analytical solutions for $u$ and $v$

According to the definition of $b_k$ in (20), it can be rewritten in terms of $u$ and $v$

$$b_k = ug_{1k} + vg_{2k} \tag{30}$$

where

$$g_{1k} = \sqrt{\frac{2\Delta t}{N}} \sum_{j=1}^{N} g_1(t_j) \exp[-2\pi \mathbf{i} \frac{(k-1)(j-1)}{N}] \qquad (k = 1,..., N) \tag{31}$$

$$g_{2k} = \sqrt{\frac{2\Delta t}{N}} \sum_{j=1}^{N} g_2(t_j) \exp[-2\pi \mathbf{i} \frac{(k-1)(j-1)}{N}] \qquad (k = 1,..., N) \tag{32}$$

are the FFT of $g_1$ and $g_2$, respectively.

Note that $g_{1k}$ and $g_{2k}$ are complex numbers. They can be expressed as

$$g_{1k} = g_{1k}^{\mathrm{R}} + \mathbf{i} g_{1k}^{\mathrm{I}} \tag{33}$$

$$g_{2k} = g_{2k}^{\mathrm{R}} + \mathbf{i} g_{2k}^{\mathrm{I}} \tag{34}$$

where $g_{1k}^{\mathrm{R}}$, $g_{1k}^{\mathrm{I}}$, $g_{2k}^{\mathrm{R}}$ and $g_{2k}^{\mathrm{I}}$ are all real numbers. Then

$$b_{\mathrm{R}k} = \mathrm{Re}\, b_k = u g_{1k}^{\mathrm{R}} + v g_{2k}^{\mathrm{R}} \tag{35}$$

$$b_{\mathrm{I}k} = \mathrm{Im}\, b_k = u g_{1k}^{\mathrm{I}} + v g_{2k}^{\mathrm{I}} \tag{36}$$

Substituting (35) and (36) into (21), differentiating with respect to $u$ and setting it equal to zero gives

$$\begin{aligned} & u \sum_k (1-a_k)[(g_{1k}^{\mathrm{R}})^2 + (g_{1k}^{\mathrm{I}})^2] + v \sum_k (1-a_k)(g_{1k}^{\mathrm{R}} g_{2k}^{\mathrm{R}} + g_{1k}^{\mathrm{I}} g_{2k}^{\mathrm{I}}) \\ & = \boldsymbol{\varphi}^T \sum_k (1-a_k)(g_{1k}^{\mathrm{R}}\, \mathrm{Re}\, \mathcal{F}_k + g_{1k}^{\mathrm{I}}\, \mathrm{Im}\, \mathcal{F}_k) \end{aligned} \tag{37}$$

A similar operation for $v$ gives

$$\begin{aligned} & u \sum_k (1-a_k)(g_{1k}^{\mathrm{R}} g_{2k}^{\mathrm{R}} + g_{1k}^{\mathrm{I}} g_{2k}^{\mathrm{I}}) + v \sum_k (1-a_k)[(g_{2k}^{\mathrm{R}})^2 + (g_{2k}^{\mathrm{I}})^2] \\ & = \boldsymbol{\varphi}^T \sum_k (1-a_k)(g_{2k}^{\mathrm{R}}\, \mathrm{Re}\, \mathcal{F}_k + g_{2k}^{\mathrm{I}}\, \mathrm{Im}\, \mathcal{F}_k) \end{aligned} \tag{38}$$

Solving (37) and (38) simultaneously for $u$ and $v$ gives their MPVs

$$\hat{u} = \frac{c_{13} c_{22} - c_{12} c_{23}}{c_{11} c_{22} - c_{12} c_{21}} \tag{39}$$

$$\hat{v} = \frac{c_{11}c_{23} - c_{13}c_{21}}{c_{11}c_{22} - c_{12}c_{21}} \tag{40}$$

where

$$c_{11} = \sum_k (1-a_k)[(g_{1k}^{\mathrm{R}})^2 + (g_{1k}^{\mathrm{I}})^2] \tag{41}$$

$$c_{12} = c_{21} = \sum_k (1-a_k)(g_{1k}^{\mathrm{R}} g_{2k}^{\mathrm{R}} + g_{1k}^{\mathrm{I}} g_{2k}^{\mathrm{I}}) \tag{42}$$

$$c_{13} = \boldsymbol{\varphi}^T \sum_k (1-a_k)(g_{1k}^{\mathrm{R}} \operatorname{Re}\mathcal{F}_k + g_{1k}^{\mathrm{I}} \operatorname{Im}\mathcal{F}_k) \tag{43}$$

$$c_{22} = \sum_k (1-a_k)[(g_{2k}^{\mathrm{R}})^2 + (g_{2k}^{\mathrm{I}})^2] \tag{44}$$

$$c_{23} = \boldsymbol{\varphi}^T \sum_k (1-a_k)(g_{2k}^{\mathrm{R}} \operatorname{Re}\mathcal{F}_k + g_{2k}^{\mathrm{I}} \operatorname{Im}\mathcal{F}_k) \tag{45}$$

Thus, the MPV of $u$ and $v$ can be expressed in terms of the remaining modal parameters to be identified. During numerical optimization these two quantities can be obtained once other modal parameters are optimized.

## 3.4. Low channel noise approximation

Before we present the algorithm for calculating the MPV of modal parameters we study the asymptotic behavior of the MPV when the channel noise is small, in the sense that $S_e / SD_k << 1$. It turns out that in this case closed-form expressions for the MPV are available for some of the modal parameters. These can be used as initial guesses for the fast algorithm to be presented in the next subsection.

When $S_e / SD_k << 1$, we have

$$a_k \sim 1 - S_e / SD_k \tag{46}$$

$$\mathbf{A} \sim \mathbf{A}_0 - S_e S^{-1} \sum_k D_k^{-1} \mathbf{D}_k \tag{47}$$

where

$$\mathbf{A}_0 = \sum_k \mathbf{D}_k \tag{48}$$

$$\mathbf{D}_k = \mathrm{Re}\mathcal{F}_k \,\mathrm{Re}\mathcal{F}_k^T + \mathrm{Im}\mathcal{F}_k \,\mathrm{Im}\mathcal{F}_k^T \tag{49}$$

We first investigate the asymptotic behavior of the mode shape. Note from (28) that

$$\mathbf{q} \sim S_e S^{-1} \sum_k D_k^{-1} (b_{\mathrm{R}k}\, \mathrm{Re}\mathcal{F}_k + b_{\mathrm{I}k}\, \mathrm{Im}\mathcal{F}_k) \tag{50}$$

This shows that the term $\mathbf{q}\mathbf{q}^T$ in the expression of $\mathbf{G}$ in (29) is O( $S_e^2$ ). As a result, $\mathbf{G}$ is dominated by the diagonal blocks and is thus asymptotically block-diagonal, i.e.,

$$\mathbf{G} \sim \begin{bmatrix} \mathbf{A}_0 & \\ & \mathbf{A}_0 \end{bmatrix} \tag{51}$$

This implies that the most probable mode shape will be asymptotically equal to the eigenvector of $\mathbf{A}_0$ with the largest eigenvalue.

To investigate the asymptotic MPV of $S_e$, we apply the approximations in (46) and (47) to the NLLF in (21) . This gives, to the leading order,

$$L \sim (n-1)N_f \ln S_e + S_e^{-1}(d - \boldsymbol{\varphi}^T \mathbf{A}_0 \boldsymbol{\varphi}) + \text{terms that do not depend on } S_e \tag{52}$$

As the form $a \ln x + b / x$ has a unique minimum at $x = b / a$, the asymptotic MPV of $S_e$ is given by

$$\hat{S}_e \sim \frac{d - \boldsymbol{\varphi}^T \mathbf{A}_0 \boldsymbol{\varphi}}{(n-1)N_f} \tag{53}$$

Similarly, for $S$, we note that

$$L \sim N_f \ln S + S^{-1} \sum_k D_k^{-1} [\boldsymbol{\varphi}^T \mathbf{D}_k \boldsymbol{\varphi} + b_{\mathrm{R}k}^2 + b_{\mathrm{I}k}^2 - 2\boldsymbol{\varphi}^T (b_{\mathrm{R}k}\, \mathrm{Re}\mathcal{F}_k + b_{\mathrm{I}k}\, \mathrm{Im}\mathcal{F}_k)] + \text{terms that do not depend on } S \tag{54}$$

This yields the asymptotic MPV of $S$ as

$$\hat{S} \sim N_f^{-1} \sum_k D_k^{-1} [\boldsymbol{\varphi}^T \mathbf{D}_k \boldsymbol{\varphi} + b_{\mathrm{R}k}^2 + b_{\mathrm{I}k}^2 - 2\boldsymbol{\varphi}^T (b_{\mathrm{R}k} \operatorname{Re}\mathcal{F}_k + b_{\mathrm{I}k} \operatorname{Im}\mathcal{F}_k)] \tag{55}$$

When calculating $b_{\mathrm{R}k}$ and $b_{\mathrm{I}k}$, the initial conditions $u$ and $v$ are indispensable. Applying the approximations in (46) , (41) to (45) can be written as

$$c_{11} \sim S_e S^{-1} \sum_k D_k^{-1} [(g_{1k}^{\mathrm{R}})^2 + (g_{1k}^{\mathrm{I}})^2] \tag{56}$$

$$c_{12} = c_{21} \sim S_e S^{-1} \sum_k D_k^{-1} (g_{1k}^{\mathrm{R}} g_{2k}^{\mathrm{R}} + g_{1k}^{\mathrm{I}} g_{2k}^{\mathrm{I}}) \tag{57}$$

$$c_{13} \sim S_e S^{-1} \boldsymbol{\varphi}^T \sum_k D_k^{-1} (g_{1k}^{\mathrm{R}} \operatorname{Re}\mathcal{F}_k + g_{1k}^{\mathrm{I}} \operatorname{Im}\mathcal{F}_k) \tag{58}$$

$$c_{22} \sim S_e S^{-1} \sum_k D_k^{-1} [(g_{2k}^{\mathrm{R}})^2 + (g_{2k}^{\mathrm{I}})^2] \tag{59}$$

$$c_{23} \sim S_e S^{-1} \boldsymbol{\varphi}^T \sum_k D_k^{-1} (g_{2k}^{\mathrm{R}} \operatorname{Re}\mathcal{F}_k + g_{2k}^{\mathrm{I}} \operatorname{Im}\mathcal{F}_k) \tag{60}$$

Substituting (56) to (60) into (39) and (40), after algebra, the asymptotic MPV $\hat{u}$ and $\hat{v}$ can be determined. The solution does not depend on $S$ or $S_e$, because the factor $S_e S^{-1}$ appears in all $c_{ij} (i = 1,2; j = 1,2,3)$ and so will be cancelled out in (39) and (40).

Some comments regarding the asymptotic expressions are in order. The asymptotic MPV for $\boldsymbol{\varphi}$ depends only on the data and so it can be calculated directly from the data. The same is also true for $S_e$. Interestingly, the asymptotic MPV of $\boldsymbol{\varphi}$ and $S_e$ are calculated in the same manner as their counterparts in ambient vibration test [34], although now the data also contains free vibration response. For $S$, $u$ and $v$, their expressions depend on the natural frequency and damping ratio.

## 3.5. Fast algorithm

The analytical MPVs of the mode shape and initial conditions in Sections 3.2 and 3.3 reduce substantially the number of variables to be numerically optimized in the MPV identification. The algorithm for obtaining the MPV of the modal parameters for a single mode in the selected frequency band is presented as follows. Recall that the modal parameters include the natural frequency $f$, damping ratio $\zeta$, mode shape $\boldsymbol{\varphi}$, PSD of modal force $S$, PSD of prediction error $S_e$, and initial conditions $u$ and $v$.

The initial guess for the natural frequency can be picked from the spectrum calculated based on the data. The initial guess for the damping ratio may be nominally taken as 1% (say). The initial guesses for the remaining parameters can be taken as the low channel noise approximations presented in Section 3.4. With these initial guesses, the MPV of $\{f, \zeta, S, S_e\}$ can be determined by numerically minimizing the NLLF in (21) under the norm constraint $\boldsymbol{\varphi}^T\boldsymbol{\varphi} = 1$. During minimization, $u$ and $v$ should be evaluated at their analytical MPVs in (39) and (40), respectively (it is suggested that they are evaluated inside the objective function in the optimization for easy convergence); $\boldsymbol{\varphi}$ should be evaluated at its analytical MPV, being equal to the first half of the eigenvector (normalized with unit norm) with the largest eigenvalue of $\mathbf{G}$ in (29). Upon convergence the MPV of $\boldsymbol{\varphi}$ can be evaluated at the MPV of $\{f, \zeta, S, S_e, u, v\}$. The flowchart of the method can be seen in Figure 1.

## 4. General multiple modes

For general multiple modes within the selected frequency band, closed-form analytical expression for the most probable mode shape has not been found. In fact, even in the case of ambient vibration data the fast algorithm developed so far is iterative [33]. Instead of developing an iterative procedure that is likely to be a cascaded and more complicated version of [33], we consider the case when the ambient vibration contribution in the data can be ignored. In this case we have been able to obtain a closed-form solution for the mode shape, leading to a fast algorithm for general multiple modes.

Significant simplification results when the ambient vibration response $\ddot{\mathbf{x}}_{aj}$ in (1) is ignored. In the Bayesian identification framework this corresponds to setting the PSD matrix of modal force to be a zero matrix, i.e.,

$$\mathbf{S} = \mathbf{0} \tag{61}$$

In this case, the matrix $\mathbf{C}_k(\boldsymbol{\theta})$ in (6) reduces to

$$\mathbf{C}_k(\boldsymbol{\theta}) = \frac{S_e}{2}\mathbf{I}_{2n} \tag{62}$$

and the NLLF in (14) reduces to

$$L(\boldsymbol{\theta}) = nN_f \ln \pi + nN_f \ln S_e + S_e^{-1}\sum_k [\mathbf{Z}_k - \boldsymbol{\mu}_k(\boldsymbol{\theta})]^T [\mathbf{Z}_k - \boldsymbol{\mu}_k(\boldsymbol{\theta})] \tag{63}$$

We next write the summand in terms of the (complex-valued) FFT vector $\mathcal{F}_k \in C^n$ instead of the augmented vector $\mathbf{Z}_k = [\mathrm{Re}\mathcal{F}_k; \mathrm{Im}\mathcal{F}_k] \in R^{2n}$ as it is found to simplify algebra:

$$L(\boldsymbol{\theta}) = nN_f \ln \pi + nN_f \ln S_e + S_e^{-1}\sum_k [\mathcal{F}_k - \tilde{\mathcal{F}}_k(\boldsymbol{\theta})]^* [\mathcal{F}_k - \tilde{\mathcal{F}}_k(\boldsymbol{\theta})] \tag{64}$$

where '*' denotes the complex conjugate transpose; $\tilde{\mathcal{F}}_k(\boldsymbol{\theta})$ denotes the FFT of the theoretical free vibration acceleration $\ddot{\mathbf{x}}_{\mathrm{f}}$ in (13).

In view of the mathematical structure of the NLLF, we separate the set of modal parameters into $S_e$ and the remaining parameters $\boldsymbol{\theta}' = \{ f_i, \zeta_i, u_i, v_i : i = 1,\ldots,m; \boldsymbol{\Phi}\}$.

The NLLF can then be written as

$$L(\boldsymbol{\theta}', S_e) = nN_f \ln \pi + nN_f \ln S_e + S_e^{-1} J(\boldsymbol{\theta}') \tag{65}$$

where

$$J(\boldsymbol{\theta}') = \sum_k [\mathcal{F}_k - \tilde{\mathcal{F}}_k(\boldsymbol{\theta}')]^* [\mathcal{F}_k - \tilde{\mathcal{F}}_k(\boldsymbol{\theta}')] \tag{66}$$

Direct minimization of $L(\boldsymbol{\theta}', S_e)$ with respect to $S_e$ yields its MPV as

$$\hat{S}_e = \frac{J(\boldsymbol{\theta}')}{nN_f} \tag{67}$$

This equation shows that the MPV of $S_e$ can be calculated when the MPV of other modal parameters are known. On the other hand, as $L(\boldsymbol{\theta}', S_e)$ depends on $\boldsymbol{\theta}'$ only through $J(\boldsymbol{\theta}')$, it can be easily seen from (65) that the derivative of $L(\boldsymbol{\theta}', S_e)$ with respect to $\boldsymbol{\theta}'$ is equal to that of $J(\boldsymbol{\theta}')$ multiplied by $S_e^{-1}$. This means that the MPV of $\boldsymbol{\theta}'$ can be obtained by minimizing $J(\boldsymbol{\theta}')$ regardless of $S_e$.

### 4.1. Most probable value for $\{f_i, \zeta_i, u_i, v_i : i = 1,...,m;\ \mathbf{\Phi}\}$

As usual, the dependence of the $J(\boldsymbol{\theta}')$ and hence the NLLF on $f_i$ or $\zeta_i$ is implicitly nonlinear and so their MPV often need to be found by brute-force numerical optimization. However, it turns out that it is possible to obtain partial analytical solutions for the MPV of $\{u_i, v_i\}$ and $\mathbf{\Phi}$. This can be done by combining the initial condition and normalized mode shape into an unconstrained vector. The details are as follows.

Let $u_i$ and $v_i$ be parameterized as

$$u_i = c_i \sin\alpha_i \tag{68}$$

$$v_i = c_i \cos\alpha_i \tag{69}$$

Note that $c_i$ and $\alpha_i$ can be easily recovered from $u_i$ and $v_i$:

$$c_i = \sqrt{u_i^2 + v_i^2} \tag{70}$$

$$\alpha_i = \tan^{-1}\frac{u_i}{v_i} \tag{71}$$

On the other hand, let

$$\mathbf{\Phi}_c(i) = c_i \mathbf{\Phi}(i) \in R^n \tag{72}$$

Since the norm of $\mathbf{\Phi}(i)$ is equal to 1, i.e., $\|\mathbf{\Phi}(i)\| = 1$, $\|\mathbf{\Phi}_c(i)\| = c_i$ and so $\mathbf{\Phi}_c(i)$ is unconstrained. In terms of $\mathbf{\Phi}_c(i)$, $\tilde{\mathcal{F}}_k(\boldsymbol{\theta}')$ can be represented as

$$\tilde{\mathcal{F}}_k(\boldsymbol{\theta}') = \sum_{i=1}^{m} \bar{b}_{ik} \mathbf{\Phi}_c(i) \tag{73}$$

where

$$\bar{b}_{ik} = \sqrt{\frac{2\Delta t}{N}} \sum_{j=1}^{N} [g_{1i}(t_j)\sin\alpha_i + g_{2i}(t_j)\cos\alpha_i] \exp[-2\pi \mathbf{i} \frac{(k-1)(j-1)}{N}] \quad (k = 1,..., N) \tag{74}$$

is a normalized counterpart of $b_{ik}$ (defined in (20) with the mode index '$i$' added).

Using the representation of $\tilde{\mathcal{F}}_k(\boldsymbol{\theta}')$ in (73), the set of modal parameters becomes

$$\boldsymbol{\theta}' = \{f_i, \zeta_i, \alpha_i :\ i = 1,...,m;\ \mathbf{\Phi}_c \in R^{n\times m}\} \tag{75}$$

and there is no longer any constraint.

We next derive an analytical solution for the MPV of $\mathbf{\Phi}_c(i)$ $(i=1,...,m)$ so that eventually only the remaining parameters $\{f_i,\zeta_i,\alpha_i: i=1,...,m\}$ need to be numerically optimized.

To facilitate derivation of the most probable mode shapes, we re-write (73) in a compact form:

$$\tilde{\mathcal{F}}_k(\boldsymbol{\theta}')=[\bar{b}_{1k}\mathbf{I}_n,...,\bar{b}_{mk}\mathbf{I}_n]\begin{bmatrix}\mathbf{\Phi}_c(1)\\ \vdots \\ \mathbf{\Phi}_c(m)\end{bmatrix}=(\bar{\mathbf{b}}_k\otimes\mathbf{I}_n)(\mathbf{\Phi}_c:) \tag{76}$$

where

$$\bar{\mathbf{b}}_k=[\bar{b}_{1k},...,\bar{b}_{mk}] \tag{77}$$

is a complex 1-by-m row vector; '$\otimes$' denotes the Kronecker product; $(\mathbf{\Phi}_c:)\in R^{nm}$ denotes the 'vectorization' of $\mathbf{\Phi}_c=[\mathbf{\Phi}_c(1),...,\mathbf{\Phi}_c(m)]\in R^{n\times m}$ formed by stacking column-wise its columns, i.e.,

$$(\mathbf{\Phi}_c:)=\begin{bmatrix}\mathbf{\Phi}_c(1)\\ \vdots \\ \mathbf{\Phi}_c(m)\end{bmatrix} \tag{78}$$

Substituting (76) into (66) gives a quadratic form in $(\mathbf{\Phi}_c:)$:

$$J(\boldsymbol{\theta}')=(\mathbf{\Phi}_c:)^T\mathbf{Q}_1(\{f_i,\zeta_i,\alpha_i\})(\mathbf{\Phi}_c:)-2(\mathbf{\Phi}_c:)^T\mathbf{Q}_2(\{f_i,\zeta_i,\alpha_i\})+\sum_k\mathcal{F}_k^*\mathcal{F}_k \tag{79}$$

where

$$\mathbf{Q}_1(\{f_i,\zeta_i,\alpha_i\})=[\sum_k\mathrm{Re}(\bar{\mathbf{b}}_k^*\bar{\mathbf{b}}_k)]\otimes\mathbf{I}_n\in R^{mn\times mn} \tag{80}$$

$$\mathbf{Q}_2(\{f_i,\zeta_i,\alpha_i\})=\sum_k\mathrm{Re}[(\bar{\mathbf{b}}_k\otimes\mathbf{I}_n)^*\mathcal{F}_k]=\sum_k\mathrm{Re}(\bar{\mathbf{b}}_k^*\otimes\mathcal{F}_k)\in R^{mn} \tag{81}$$

As a standard result in linear algebra, minimizing the quadratic form in (79) with respect to $(\mathbf{\Phi}_c:)$ yields the most probable mode shape in vectorized form:

$$(\hat{\mathbf{\Phi}}_c:)=\mathbf{Q}_1(\{f_i,\zeta_i,\alpha_i\})^{-1}\mathbf{Q}_2(\{f_i,\zeta_i,\alpha_i\}) \tag{82}$$

Note that $\mathbf{Q}_1$ and $\mathbf{Q}_2$ depend on $\{f_i, \zeta_i, \alpha_i\}$ and so will $(\hat{\mathbf{\Phi}}_c :)$ in (82).

After the MPV of $(\mathbf{\Phi}_c :)$ has been obtained, the MPV of $c_i$ can be determined as

$$\hat{c}_i = \left\| \hat{\mathbf{\Phi}}_c(i) \right\| \qquad (i = 1, \ldots, m) \tag{83}$$

The most probable mode shape normalized to unity is given by

$$\hat{\mathbf{\Phi}}(i) = \left\| \hat{\mathbf{\Phi}}_c(i) \right\|^{-1} \hat{\mathbf{\Phi}}_c(i) \qquad (i = 1, \ldots, m) \tag{84}$$

Evaluating $J(\boldsymbol{\theta}')$ at the most probable mode shape $(\hat{\mathbf{\Phi}}_c :)$ gives a function in terms of only $\{f_i, \zeta_i, \alpha_i\}$, which can be further minimized to yield their MPVs:

$$J(\{f_i, \zeta_i, \alpha_i\}) = (\sum_k \mathcal{F}_k^* \mathcal{F}_k) - \mathbf{Q}_2(\{f_i, \zeta_i, \alpha_i\})^T \mathbf{Q}_1(\{f_i, \zeta_i, \alpha_i\})^{-1} \mathbf{Q}_2(\{f_i, \zeta_i, \alpha_i\}) \tag{85}$$

where the dependence of $\mathbf{Q}_1$ and $\mathbf{Q}_2$ on $\{f_i, \zeta_i, \alpha_i\}$ have been emphasized. Note that the first term on the RHS of (85) is a constant, and so it need not be calculated during numerical optimization. The number of parameters that need to be optimized is only $3m$, which does not depend on the number of measured dofs $n$.

## 4.2. Fast algorithm

The algorithm for obtaining the MPV of modal parameters for general multiple modes in the selected frequency band (ignoring ambient vibration in the identification model) is presented as follows. Recall that the modal parameters in this case are the natural frequencies $\{f_i\}$, damping ratios $\{\zeta_i\}$, initial conditions $\{u_i, v_i\}$ $(i = 1, \ldots, m)$, PSD of prediction error $S_e$ and mode shape matrix $\mathbf{\Phi} \in R^{n \times m}$ (with each column normalized to unity). The algorithm only involves numerical optimization of $\{f_i, \zeta_i, \alpha_i\}$, where $\{\alpha_i\}$ is involved in the parameterization of $\{u_i, v_i\}$ in (68) and (69). The MPV of the remaining parameters is recovered later.

As in Section 3.5, the initial guesses for the natural frequencies $\{f_i\}$ can be picked from the spectrum calculated based on the data. The initial guesses of the damping ratios $\{\zeta_i\}$ may be nominally taken as 1% (say). The initial guesses for $\{\alpha_i\}$ can be taken uniformly random on $[0,\ 2\pi]$.

1. Determine the MPV of $\{f_i, \zeta_i, \alpha_i : i = 1,...,m\}$ by numerically minimizing $J$ in (85).
2. Determine the MPV of $\{\mathbf{\Phi}_c(i) : i = 1,...,m\}$ from (82), where $\{f_i, \zeta_i, \alpha_i :\ i = 1,...,m\}$ are evaluated at their MPVs obtained in Step 1.
3. Determine the MPV of $\{c_i\}$ from (83); the MPV of $\{u_i, v_i\}$ from (68) and (69), respectively; the MPV of $\mathbf{\Phi}$ from (84); and the MPV of $S_e$ from (67).

The flowchart of the method is shown in Figure 2.

## 5. Conclusions

A frequency-domain Bayesian framework for modal identification has been developed to identify the most probable values (MPVs) of modal parameters using free vibration data. Due to the computational difficulties in the process of optimization, two different cases are considered to determine the MPVs efficiently. The first one considers the ambient vibration data in the model, but is only applicable for well-separated modes. The second case ignores the ambient vibration and models it as prediction error, but it is applicable to general multiple (possibly closely-spaced) modes. In both cases, analytical solutions for the mode shapes have been obtained in terms of other parameters, so that the growth of computational effort with the number of measured dofs is effectively suppressed. When ambient response is ignored, the likelihood function can be simplified significantly, but when the free vibration response is relatively small compared with the ambient vibration, there may be some effect on the identified results, which will be investigated in the companion paper. The companion paper also investigates the posterior uncertainty of the modal parameters in terms of their posterior covariance matrix. It verifies the developed methods and applies them to field test data as well.

## Acknowledgements

The work described in this paper is partially supported by Fundamental Research Funds for the Central Universities, China (Grant No. 2014KJ040), Grant EGG10034 from the University of

Liverpool and a grant from the Research Grants Council of the Hong Kong Special Administrative Region, China (Project No. 9041758 (CityU 110012)).

## References

[1] H. Sohn, J. Czarnecki, C. Farrar, Structural health monitoring using statistical process control, Journal of Structure Engineering 126(11) (2000) 1356–1363.

[2] H. Sohn, C.R. Farrar, F.M. Hemez, D.D. Shunk, D.W. Stinemates, B.R. Nadler, A Review of Structural Health Monitoring Literature: 1996-2001. Los Alamos National Laboratory Report, LA-13976-MS, 2003.

[3] J.M. Ko, Y.Q. Ni, Technology developments in structural health monitoring of large-scale bridges, Engineering Structures 27 (2005) 1715–1725.

[4] G. H. James, T. G. Carne, J. P. Lauffer, The natural excitation technique (NExT) for modal parameter extraction from operating structures, International Journal Analytical Experimental Modal Analysis 10(2) (1995) 260 – 277.

[5] J. M.W. Brownjohn, Ambient vibration studies for system identification of tall buildings, Earthquake Engineering and Structural Dynamics 32(2003) 71-95.

[6] S.K. Au, F.L. Zhang,Y.C. Ni, Bayesian operational modal analysis: theory, computation, practice, Computers and Structures 126(2013) 3-14.

[7] I. Okauchi, T. Miyata, M. Tatsumi, N, Sasaki, Field vibration test of a long span cable-stayed bridge using large exciters, Structural Engineering 14 (1) (1997) 83-93.

[8] A. De Sortisa, E. Antonaccib, F. Vestronic, Dynamic identification of a masonry building using forced vibration tests, Engineering Structures 27 (2005) 255-265.

[9] J. M.W. Brownjohn, A. Pavic, Experimental methods for estimating modal mass in footbridges using human-induced dynamic excitation, Engineering Structures 29 (2007) 2833–2843.

[10] S.K. Au, Y.C. Ni, F.L. Zhang, H.F. Lam, Full-scale dynamic testing and modal identification of a coupled floor slab system, Engineering Structures 37 (2012) 167-178.

[11] W. Zhou, D. Chelidze, Generalized Eigenvalue Decomposition in Time Domain Modal Parameter Identification, Journal of Vibration and Acoustics 130 (2007) 011001-1-011001-6.

[12] S. R. Ibrahim, E. C. Mikulcik, A Time Domain Modal Vibration Test Technique, Bulletin of Shock and Vibration 43(4) (1973) 21–37.

[13] S.R. Ibrahim, E.C. Mikulcik, A method for direct identification of vibration parameters from the free responses, Bulletin of Shock and Vibration 47(4) (1977) 183–198.

[14] D. Brown, R. Allemang, R. Zimmerman, M. Mergeay, Parameter estimation techniques for modal analysis, SAE Transaction 88(1) (1979) 828–846.

[15] S.K. Au, C.T. Hg, H.W. Sien, H.Y. Chua, Modal identification of a suspension footbridge using free vibration signatures, International Journal of Applied Mathematics and Mechanics 1(4) (2005) 55-73.

[16] J.L. Beck, Determining models of structures from earthquake records Report No. EERL 78-01, California Institute of Technology, Earthquake Engineering Research Laboratory, Pasadena, California (1978).

[17] B.F. Feeny, R. Kappagantu, On the physical interpretation of proper orthogonal modes in vibration, Journal of Sound and Vibration 211 (1998) 607–616.

[18] G. Kerschen, J.G. Golinval, Physical interpretation of the proper orthogonal modes using the singular value decomposition, Journal of Sound and Vibration 249 (2002) 849–865.

[19] S. Han, B. Feeny, Application of proper orthogonal decomposition to structural vibration analysis, Mechanical System and Signal Processing 17 (2003) 989–1001.

[20] B.T. Wang, D.K. Cheng, Modal analysis of mdof system by using free vibration response data only, Journal of Sound and Vibration 311 (2008) 737–755.

[21] B.T. Wang, D.K. Cheng, Modal analysis by free vibration response only for discrete and continuous systems, Journal of Sound and Vibration 330 (16) (2011) 3913–3929.

[22] M. Ruzzene, A. Fasana, L. Garibaldi, B. Piombo, Natural frequencies and dampings identification using wavelet transform: application to real data, Mechanical System and Signal Processing 11 (2) (1997) 207–218.

[23] C.S. Huang, S.L. Hung, C.I. Lin, W.C. Su, A wavelet-based approach to identifying structural modal parameters from seismic response and free vibration data, Computer-Aided Civil and Infrastructure Engineering 20 (2005) 408–423.

[24] S. Gouttebroze, J. Lardies, On using the wavelet transform in modal analysis, Mechanics Research Communications 28 (5) (2001) 561–569.

[25] J. Lardies, S. Gouttebroze, Identification of modal parameters using the wavelet transform, International Journal of Mechanical Sciences 44 (11) (2002) 2263–2283.

[26] T.P. Le, P. Argoul, Continuous wavelet transform for modal identification using free

decay response, Journal of Sound and Vibration 277 (2004) 73–100.

[27] N.E. Huang, Z. Shen, S.R. Long, M.C. Wu, et al, The empirical mode decomposition and the Hilbert spectrum for nonlinear and non-stationary time series analysis. Proceedings of the royal society of London, series a: mathematical, physical and engineering sciences 454 (1998) 903–995.

[28] M. Feldman, Non-linear free vibration identification via the Hilbert Transform. Journal of Sound and Vibration 208(3) (1997) 475–489.

[29] J.P. Han, P.J. Zheng, H.T. Wang, Structural modal parameter identification and damage diagnosis based on Hilbert-Huang transform, Earthquake Engineering and Engineering Vibration 13 (2014) 101-111.

[30] K.V. Yuen and L. S. Katafygiotis, Bayesian fast Fourier transform approach for modal updating using ambient data. Advances in Structural Engineering 6(2) (2003) 81–95.

[31] S.K. Au, F.L. Zhang and Y.C. Ni, Bayesian operational modal analysis: Theory, computation, practice. Computers and Structures 126 (2013) 3-14.

[32] J. Schoukens, R. Pintelon, Identification of Linear Systems: A Practical Guideline for Accurate Modeling. Pergamon Press, London, 1991.

[33] S.K. Au, Fast Bayesian ambient modal identification in the frequency domain, part I: most probable value, Mechanical Systems and Signal Processing 26 (2012) 60-75.

[34] S.K. Au, Fast Bayesian FFT method for ambient modal identification with separated modes, Journal of Engineering Mechanics 137(3) (2011) 214-226.

[35] W. Gander, Least squares with a quadratic constraint, Numerische Mathematik 36 (1980) 291-307.

[36] W. Gander, G.H. Golub, U.V. Matt, A constrained eigenvalue problem, Linear Algebra and its Applications 114(115) (1989) 815-839.

[37] S.K. Au, Assembling mode shapes by least squares, Mechanical Systems and Signal Processing 25(1) (2011) 163-179.

## Figure Captions

Figure 1 Flowchart of well-separated mode case

Figure 2 Flowchart of general multiple modes case

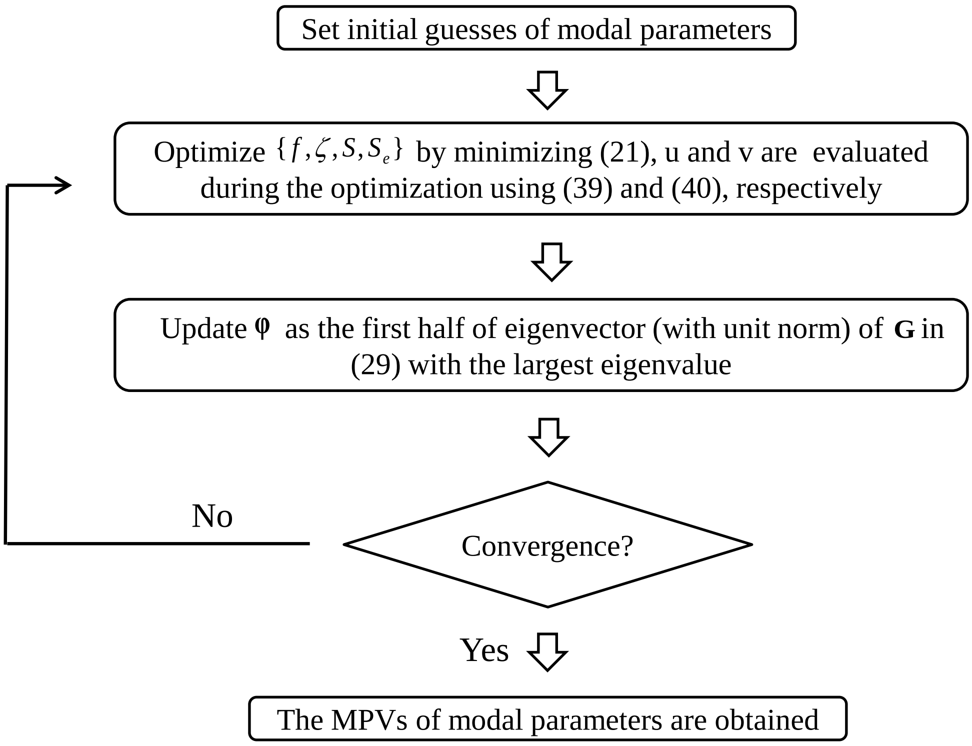


Figure 1 Flowchart of well-separated mode case

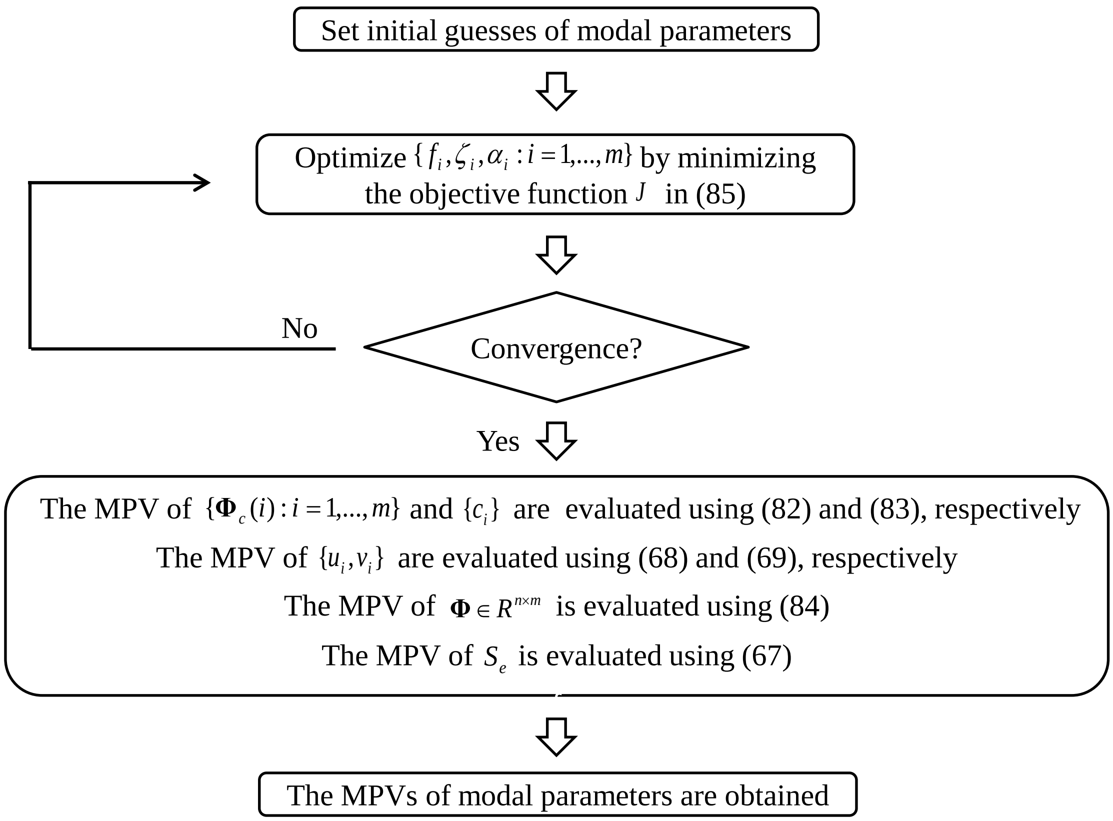


Figure 2 Flowchart of general multiple modes case